

The Effects of PWM With High dv/dt on Partial Discharge and Lifetime of Medium-Frequency Transformer for Medium-Voltage (MV) Solid State Transformer Applications

Rachit Agarwal , Member, IEEE, Hui Li , Fellow, IEEE, Zhehui Guo , Student Member, IEEE, and Peter Cheetham , Member, IEEE

Abstract—The medium-frequency (MF) transformer in a phase-shift modulated dc solid state transformer (SST) is prone to partial discharge (PD) that impacts the system reliability and lifetime. Tightly packed MF transformer windings carrying pulsewidth modulation (PWM) voltages create favorable conditions for PD inception due to proximity between adjacent winding conductors and electric field enhancement because of spiral geometry. A peak potential condition is created between the adjacent posterior conductors of the primary and secondary windings as a result of phase-shifted modulation. This along with fast alternating electric fields incepts PD at lower than expected operating voltages. Early inception of PD leads to premature transformer failure leading to unanticipated dc SST downtime. The effects of PWM voltages containing high dv/dt switching transients on PD and lifetime characteristics of MF transformer in a dc SST are not yet understood, which is investigated in this article. A nonintrusive PD detection strategy for MF PWM ac voltage is presented using high-speed optical sensors. PD characterization is performed on Kapton polyimide insulated copper foil windings for a foil-type MF transformer. Winding samples are stress tested with steady state PWM voltages up to 2 kV and frequencies up to 50 kHz with high dv/dt up to 60 V/ns generated by a half-bridge inverter using 3.3 kV SiC devices while maintaining the transformer's geometric profile. Accelerated dielectric lifetime characterization is also performed and novel lifetime prediction models are derived based on the acquired results containing both frequency and dv/dt dependent variables.

Index Terms—Medium-frequency (MF) transformer, medium-voltage (MV), partial discharge (PD), pulsewidth

Manuscript received 25 October 2021; revised 7 February 2022 and 10 April 2022; accepted 29 April 2022. Date of publication 17 May 2022; date of current version 12 December 2022. (Corresponding author: Hui Li.)

Rachit Agarwal, Zhehui Guo, and Peter Cheetham are with the Center for Advanced Power Systems, Florida State University, Tallahassee, FL 32310 USA (e-mail: ra15f@my.fsu.edu; zg18b@fsu.edu; cheetham@caps.fsu.edu).

Hui Li is with the Department of Electrical and Computer Engineering, Florida State University, Tallahassee, FL 32310 USA (e-mail: hli@caps.fsu.edu).

Color versions of one or more figures in this article are available at <https://doi.org/10.1109/TIE.2022.3174243>.

Digital Object Identifier 10.1109/TIE.2022.3174243

modulation (PWM), SiC, solid state transformer (SST), transformer lifetime.

I. INTRODUCTION

LEVERAGING the high voltage and high-speed capability of emerging wide band gap semiconductor devices, medium-voltage (MV) solid state transformer (SST) is gaining widespread applications in medium-voltage dc (MVdc) distribution, renewable energy collection, and fast charging stations. Medium-frequency (MF) transformer is crucial in an MV SST converter architecture to achieve galvanic isolation, high power density, and high efficiency.

One primary design challenge of MF transformer is to implement desired insulation at MV pulsewidth modulation (PWM) excitation without compromising on power density and efficiency. Onset of partial discharge (PD) is an indication of insulation issues in ac systems. Every discharge event reduces the insulation lifetime by degrading the insulation material leading to premature insulation failure.

Research works in [1] and [2] designed MF frequency transformers for inductor tank based MV dc SST with PWM frequency from 3 to 20 kHz. The insulation material of the windings is presented but the insulation performance remains untested. Zhao *et al.* in [3] designed a 500-kHz transformer with PTFE polymer based insulation that has been characterized up to 30 kV with short impulse voltage testing. Guo *et al.* developed a 200-kW, 15-kHz dual active bridge SST MF transformer in [4] with PD characterization up to 7.5 kV peak. The PD test is performed at 60 Hz sine ac voltage bearing different properties compared to PWM voltage. It is reported in [5] that PD is heavily influenced by the voltage shape and PWM voltage with switching transients show stronger PD activity compared to sine and triangle voltages. The PDs research for motor windings under actual PWM excitation at greater than 60 Hz frequency has been reported in [6]–[9]. However, the research of PWM effects on PD of MF transformer within SST has not been reported. The PD characteristics in SST transformer are different from that of motor winding because of difference in PWM voltage,

winding geometry, and electric field distribution between motor and transformer. SST transformer windings are subjected to greater potential difference and faster alternating electric fields between the primary and secondary side of the transformer as a consequence of phase-shift modulation and high switching frequency of SST.

MF transformer is important for dc SST's reliability since winding insulation failure can lead to short circuit fault between the high voltage and low voltage side. A survey of the literature suggests that degradation of dielectric material is affected by PD activity and the life expectancy is substantially reduced in the presence of PD [10]. Singh *et al.* [11] experimentally evaluated the lifetime of high-voltage direct current (HVdc) converter's line frequency transformer insulation under different ac voltage waveform patterns. The results show that insulation lifetime depends drastically on waveform pattern reducing the lifetime to less than one year for square voltage pattern, whereas the lifetime is greater than 40 years for sinusoidal voltage. They have performed accelerated breakdown (BD) tests on oil in paper insulation material but have not characterized the material for PDs. Insulation lifetime is heavily dependent on ac frequency primarily due to the repetitive nature of PD events following the rise and fall of alternating voltage. However, the PD effects on transformer lifetime have not been studied in [11]. Laghari and Cygan [12] show that the lifetime of polyimide Kapton film insulation is significantly reduced when ac frequency is increased to 400 Hz from 60 Hz. The failure mechanism and method for failure assessment have not been reported for MF PWM transformers.

This article studied the effect of PWM with high dv/dt switching transients on PD and lifetime characteristics of an MF transformer for MV SST especially when SiC devices are applied. The tightly packed MF transformer windings carrying high-frequency PWM voltages with high dv/dt are more prone to PDs, which may lead to premature transformer failure leading to dc SST down-time. Hence, characterization of PDs and lifetime of transformer winding insulation at precise geometry and PWM voltage excitation is important. This article presents a nonintrusive PD characterization strategy for foil-type MF transformer under high-frequency PWM waveform using high-speed optical sensors. Kapton (polyimide) insulated foil windings are stressed with steady state PWM voltages up to 2 kV and frequencies up to 50 kHz with high dv/dt up to 60 V/ns while maintaining the transformer's geometric profile. The interwinding PD inception and extinction characteristics for foil-type MF transformer are obtained, which provides an insight of transformer lifetime. Additionally, an extended transformer lifetime model considering PWM frequency and switching dv/dt is developed from accelerated winding BD tests. The model derives a mathematical relationship of switching frequency and switching speed influence on SST transformer's lifetime.

The rest of the article is organized as follows. Section II presents the dc SST topology along with foil-type MF transformer construction. Interwinding peak potential state unique to phase-shift modulated dc SST is analyzed and electric field finite-element analysis (FEA) simulation results indicating $5\times$ electric field enhancement between the primary and secondary

winding are discussed in detail. In Section III, the transformer PD characterization methodology is addressed in detail with SiC-based variable frequency and dv/dt voltage generator. Based on optical detection method, the PD inception voltage (PDIV) and PD extinction voltage (PDEV) are characterized for wide spectrum of PWM frequency between 10 Hz and 50 kHz. Post PD characterization, the foil windings are stress tested at 2 kV PWM until BD for frequencies between 10 and 50 kHz and dv/dt of 30 and 60 V/ns. The findings are presented in Section IV. Based on the BD results, lifetime models are developed with varying frequency for a fixed dv/dt . Effect of dv/dt is quantitatively represented in the mathematical models. Extended transformer lifetime model considering switching frequency and dv/dt is also discussed in Section IV. Finally, Section V concludes this article.

II. SST CONFIGURATION AND TRANSFORMER INSULATION DISCUSSION

The dc grid technology is a promising solution to integrate a large amount of renewable energies and energy storage systems. At the transmission level, the HVdc is an emerging technology to integrate large renewable power plants. At the distribution level, MVdc grids are promising for the efficient connection of distributed renewable generation and storage systems. The dc SST that interconnects MVdc distribution grids and HVdc transmission grids therefore plays a key role in such dc grids. Fig. 1 shows a dc transformer to connect MVdc distribution grids and HVdc transmission grids using phase-shifted modulation method. The power transfer is controlled by adjusting the phase shift angle between the primary and secondary voltages of an MF transformer. The primary and secondary voltages of MF transformer are also shown in Fig. 1.

A peak potential state is created between the primary and secondary side transformer windings during the duration of phase shift. In the modulation shown in Fig. 1, $\phi = 45^\circ$ is considered for simplicity. For this application, the MF transformer is designed for a unity turns ratio. Hence, the peak interwinding potential (V_{IWP}) reaches $2\times$ the dc-link voltage V_{dc} for the duration of phase-shift in the positive half cycle between 0 and T_ϕ , mathematically represented by the following equation:

$$V_{IWP} = |V_{pri} - n \cdot V_{sec}|. \quad (1)$$

Ideally, between T_ϕ and $T_s/2$, both primary voltage V_{pri} and secondary voltage V_{sec} are at same potential due to transformer turns ratio $n = 1$, making V_{IWP} hold zero potential difference. At $T_s/2$, the negative half cycle begins, again increasing V_{IWT} to $2 \cdot V_{dc}$ between $T_s/2$ and $(T_s/2 + T_\phi)$. Hence, the winding-to-winding voltage constitutes of unipolar square wave bearing twice the switching frequency of transformer PWM voltage, width equal to the operating phase-shift angle and two times amplitude of switching transients. The fast alternating electric field between the tightly packed transformer windings significantly increases the stress on posterior edges of the windings and creates favorable conditions for PD inception as well as to accelerated insulation aging due to PD activity. PD can happen either between microvoids with the winding

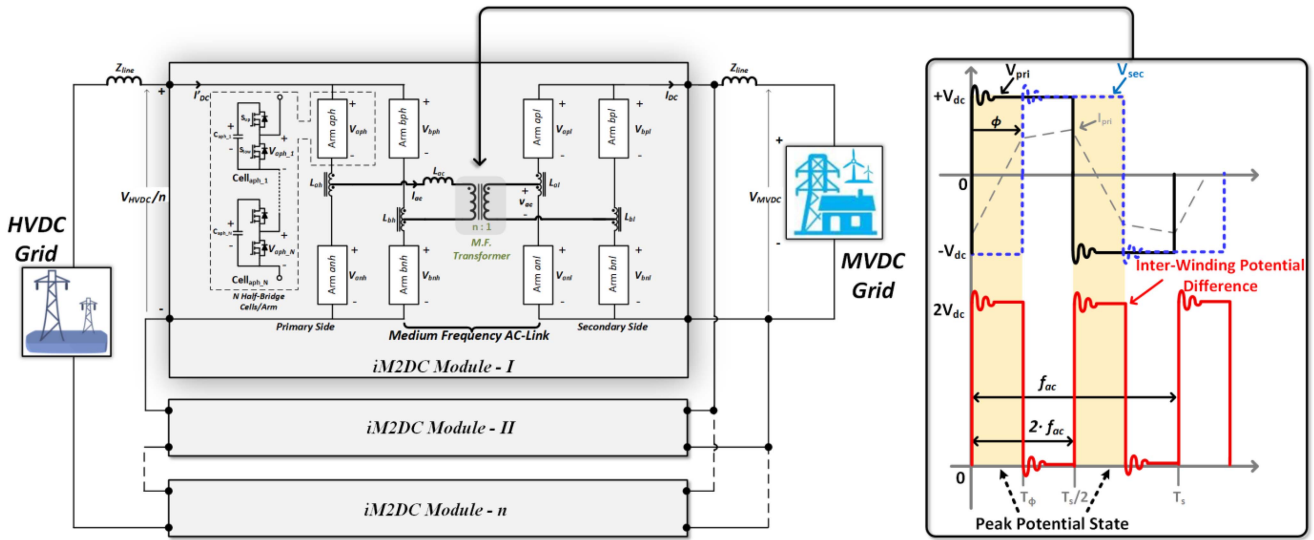


Fig. 1. SST architecture with two-level PWM voltage.

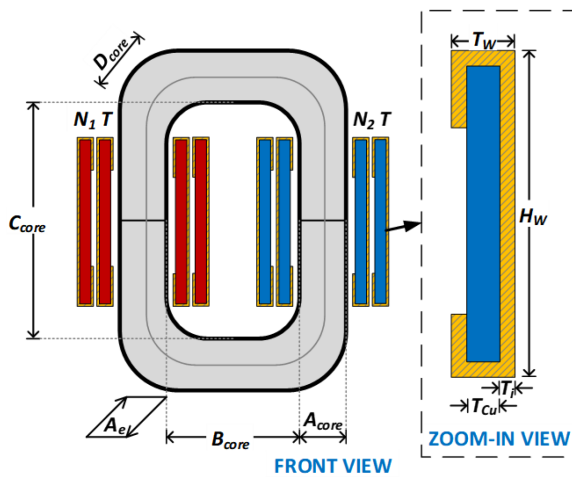


Fig. 2. Foil-type MF transformer construction.

or between the posterior insulation surfaces of primary and secondary side windings. Therefore, the interwinding insulation is challenging for phase-shifted operation based dc SST due to the peak potential state. The intrawinding insulation between two adjacent layers and the winding to core insulation is also prone to PD inception, whereas the potential difference in both cases is smaller than interwinding potential difference; hence, the focus of this work is on interwinding insulation.

An MF transformer with nanocrystalline core and copper foil windings is designed for a dc SST with phase-shifted operation to achieve high power density and low loss [13]–[15]. The transformer is structured in a UU shape with separate winding structure, as shown in Fig. 2. The windings are insulated with Kapton (polyimide) insulation because the mechanical properties of Kapton allow it to bend freely compared to other insulation materials. This allows better control over foil winding

construction, combined with thin insulation thickness improves the coupling of transformer.

Separate winding structure may suffer from higher leakage inductance due to lower magnetic coupling as compared to concentric or interleaved winding structures [4]; the separate structure however exhibits the best interwinding insulation due to natural separation between the primary and secondary sides, often aided by a small air gap. On the other hand, in interleaved winding structure, the gap between the primary and secondary side winding is minimized by directly interleaving the primary and secondary winding foil layers on top of each other to enhance the magnetic coupling. Interleaving creates the peak potential state throughout the winding length due to continuous close proximity of primary and secondary conductors wound together with no air-gap to support the dielectric strength. Consequently, the entire winding bulk is vulnerable to PD in interleaved structure, whereas only the anterior edge facing the other winding is prone to PD in separate winding structure. Hence, a separate winding structure is adopted for this work.

For transformer winding structure, PD inception depends on the electric field and dielectric strength between primary and secondary conductors. Electric field intensity is associated with the geometry and proximity of conductors carrying mismatched electric potential. The interwinding electric field severity is analyzed using 2-D axisymmetric FEA simulation on a simplified winding structure, which consists of one layer of Kapton insulation with adhesive silicone backing over 2 mil thick copper foil. The thickness of silicone and Kapton is 1 mil each. The relative permittivity of Kapton is 3.4 and that of silicone adhesive as 2.8. In this simulation, the primary side copper winding potential is set to 2 kV and the secondary side is set to 0 V to be consistent with experimental condition for PD evaluation. 0.2 mm gap distance in air represents a densely packed transformer with maximum fill factor. The zoom-in simulation results in Fig. 3 show $4 \times -5 \times$ electric field enhancements along the entire lateral edge of the primary and secondary windings. This can lead to

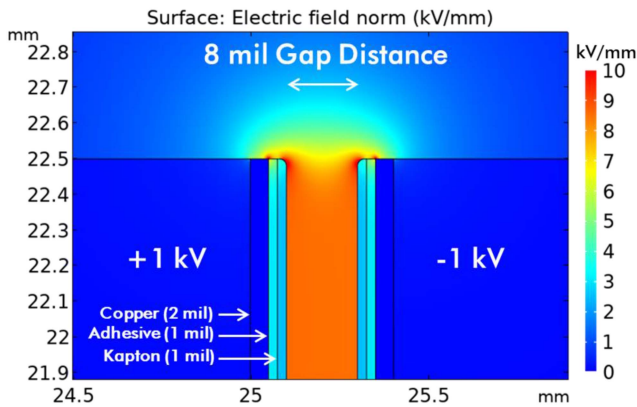


Fig. 3. FEA simulation results of the anterior winding edge with one layer of Kapton insulation.

PD inception at lower than anticipated dc-link voltages leading to unexpected transformer insulation failure. The simulation also demonstrates the edge effect predominantly enhancing the electric field at the filleted edge of the winding. Such sharp edges are a common occurrence formed during the bending and shaping process of copper metal. In addition, $\sim 2\times$ field enhancement between copper, adhesive, and Kapton creating favorable PD condition within the microcavities between the material layers.

It is important to note that fast alternating electrical field is created by the fast switching PWM voltage of the MF transformer along with the electric field enhancement leading to significant PD activity between the micro cavities as well as between the windings. In addition, the dielectric losses and unexpected local temperature rise can be expected owing to MF PWM pulses. The fast dv/dt , fast switching frequency along with switching transients can drastically reduce the lifetime of insulation in SST; the weakest point being the MF transformer interwinding insulation because it is usually designed to withstand the peak PWM voltage occurring in SST. Therefore, it is crucial to evaluate the PWM effects on PD between the interwinding insulation for MF transformer. In the following section, the interwinding PD is experimentally characterized under fast PWM voltages.

III. TRANSFORMER PD CHARACTERIZATION WITH VARIABLE SWITCHING FREQUENCY AND HIGH DV/DT

PD detection methods can be classified into electrically coupled methods and nonintrusive methods. Electrically coupled methods include the traditional coupling capacitor method where the PD activity is obtained by measuring the PD displacement current off a coupled capacitor to the specimen under test. While this method is standardized in the IEC 60270 [16] for 50/60 Hz ac PD measurement, it is unsuitable for higher frequency PWM PD measurements. Another method is ground current measurement using high frequency current transformer [17]; while this method exhibits good performance irrespective of voltage waveform shape, it suffers from severe interference due to switching inrush currents. For PWM waveform, the

inrush current overlaps the PD signal making it hard to identify. On the other hand, the nonintrusive methods include optical detection using photomultiplier tube (PMT) [8], electromagnetic detection using ultra high frequency antenna [18], as well as acoustic and electrochemical detection using ultrasound and ozone sensors. Acoustic and electrochemical detection method is based on secondary-response detection and is too slow for precise PD detection. Electromagnetic detection satisfies the detection speed requirement but the high-speed switching electromagnetic interference (EMI) interferes with the PD signal requiring extensive postprocessing to separate PD from noise. In many cases, especially at PDIV and PDEV, PD signals contain lower amplitude than EMI noise, which remains undetectable post signal processing.

The optical detection method using PMT is fully isolated from electrical disturbances. Since light is a compulsory byproduct of PD and is the fastest form of energy, PMT-based PD detection satisfies the detection speed and sensitivity requirements for MF power electronic applications. Additionally, no postprocessing of data is required, which makes it easy and compact. The PD characterization system for foil-type MF transformer is developed and shown in Fig. 4 where it consists of three main parts: 1) MF PWM generator, which is the source of PWM potential between the primary and secondary windings; 2) transformer winding test setup, which is built to hold windings under test maintaining the transformer's geometry; and 3) optical PD measuring instrument, which detects the optical photons discharged during PD event and converts it into electrical signal for acquisition. Each subcomponent is described in detail as follows.

- 1) *MF PWM Generator*: The PWM generator is shown in Fig. 4(b), which is a half-bridge inverter using discrete 3.3-kV SiC MOSFETs from GeneSiC. The maximum dc-link voltage is selected as 2 kV. Optically isolated gate drivers with desat protection drive the MOSFETs to switching frequencies up to 50 kHz, generating unipolar PWM output. The PWM frequency is varied between 10 Hz and 50 kHz. The dv/dt is limited by the parasitic capacitance associated with the winding sample and the parasitic inductance of the external current limiting resistance inserted between the PWM generator and the winding test sample. Peak dv/dt of 60 V/ns is achieved by the circuit. A second test case is attained by dropping the dv/dt to 30 V/ns by modifying the gate resistance.
- 2) *Transformer Winding Test Setup*: The detailed design parameters of this foil-type MF transformer were presented in [14]. A winding test setup is custom built in the lab with fiberglass G-10 insulating material. Since intrawinding turn-to-turn insulation is not the focus of this work, the custom test setup shown in Fig. 4(c) holds one layer of primary and one layer of secondary winding on each side while maintaining the geometry of real transformer. The winding sample is constructed with a 2 mil thick copper foil [19] shaped and layered with 3M 1093 Kapton insulation consisting of around 1 mil thick adhesive silicone backing and 1 mil of polyimide Kapton insulation. The

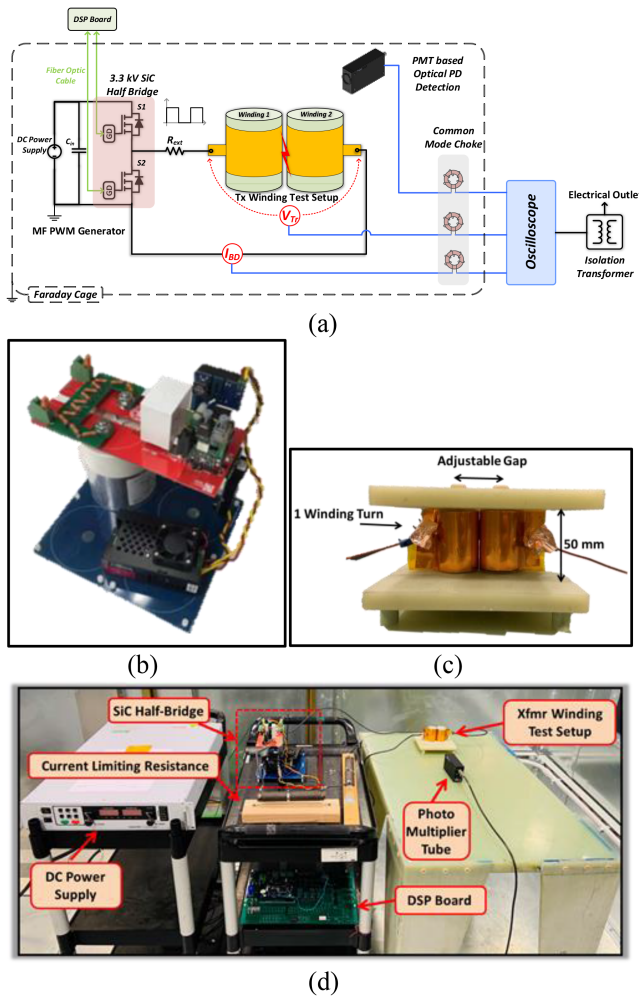


Fig. 4. (a) Schematic of the developed system to characterize PDs and lifetime of foil-type MF transformer. (b) PWM source containing SiC half-bridge, input dc-link capacitor, and optically coupled gate drivers. (c) Transformer winding test setup built with fiberglass G-10 material. (d) Photograph of PD characterization test setup inside Faraday cage.

insulation is rated to high temperature class of 180 °C and high dielectric strength of 7.5 kV.

- 3) *Optical PD Measurement*: PD is always accompanied by light radiation throughout the entire PD event from primary ionization to extinction. PMT can detect faint optical signals and the large active lens area makes it ideal to catch the scattered light from the source [20]. Hence, PMT provides high sensitivity and fast response time that is required to optically detect PDs. In addition, optical PD detection is a noninvasive technique requiring no physical voltage and current measurements from the circuit. This makes it naturally immune to the switching artifacts produced by the fast switching power electronics circuit. Hence, PD detection is possible by visualizing the raw data with no postprocessing required. Utmost care should be taken to ensure that the test area is light-free with no external sources of light that can add noise to the measurement. The optical PD measurements are validated by comparing them with the PD measurements obtained

TABLE I
TEST CASES USED FOR PD CHARACTERIZATION

Test Case	PWM Frequency	dv/dt
1	10 Hz	30 V/ns
2	100 Hz	
3	1 kHz	
4	10 kHz	
5	20 kHz	
6	30 kHz	
7	40 kHz	
8	50 kHz	
9	10 Hz	60 V/ns
10	100 Hz	
11	1 kHz	
12	10 kHz	
13	20 kHz	
14	30 kHz	
15	40 kHz	
16	50 kHz	

by Heafly coupling capacitor based PD detector at 60 Hz. Consistent results are obtained by both methods validating the authenticity of PMT-based optical PD detection.

The experimental testbed is shown in Fig. 4(d). The test is performed inside the Faraday cage facility to isolate the test circuit from switching noise and other background noises produced by the PWM source. Faraday cage is equipped with dedicated climate control equipment that maintains consistent ambient conditions of 22 °C and 28% relative humidity. The grounded Faraday cage is built with solid steel on all six faces of the room, which also provides an optical noise-free environment for accurate PD detection. PMT is placed vertically facing the adjacent edges of the primary and secondary side winding samples and PWM voltage excitation is given to the primary winding. The distance between PMT lens and winding sample is kept at approximately 6 in. The voltage across the winding is measured with a high-speed differential voltage probe. The voltage measurement is plotted against the output of the PMT to identify PD along the voltage waveform. The voltage V_{Tr} is plotted against the ground current I_{BD} during accelerated life tests. The data are visualized on an oscilloscope with 1 GHz bandwidth placed outside the Faraday cage. Common mode chokes are placed in between the long measurement leads to filter the radiated EMI noise generated by the fast switching SiC MOSFETs of the PWM generator at the rising and falling edges of the PWM voltage. The secondary side winding specimen is grounded in order to create a unipolar peak potential state identical to phase-shift modulated dc SST.

PD characterization experiments were performed on foil winding specimens under varying PWM frequency. The test scenarios are listed in Table I. For each test case, the frequency is kept constant and the voltage of the PWM generator is increased progressively until light photons are detected by the PMT. The voltage across the winding specimen and the PMT output voltage are recorded in a mixed signal oscilloscope for real-time visualization. The presence of light (discharge) is indicated by the PMT by its characteristic negative voltage pulses. PMT measurements

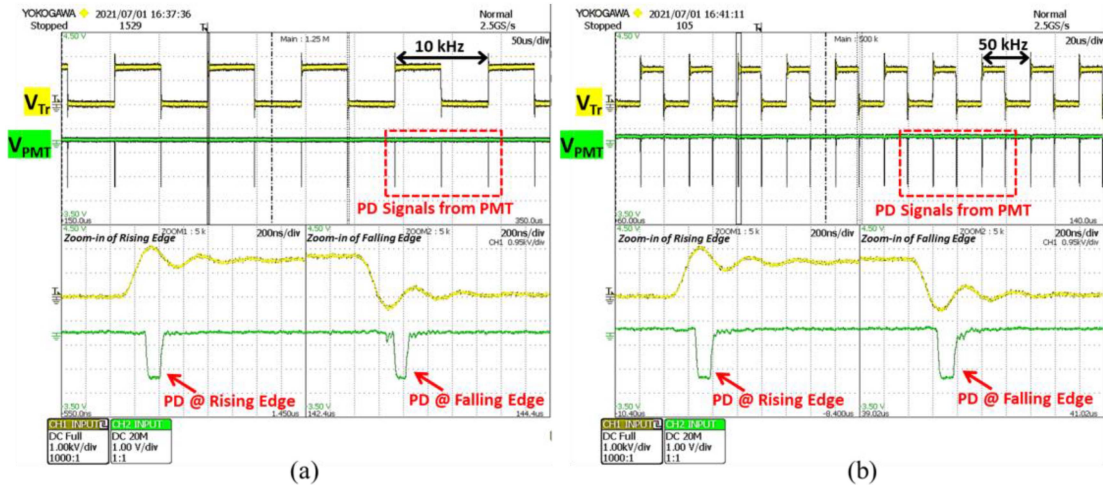


Fig. 5. PDIV measurement results with $dv/dt = 30$ V/ns at: (a) 10 kHz PWM frequency and (b) 50 kHz PWM frequency.

exhibit the periodic nature of discharge that is aligned with the rising and falling edge of the PWM voltage pulse, thus proving that the measured light is PD. The MF PWM generator voltage at which PD inception is recorded as PDIV.

PDIV measurements at 10 kHz PWM and 50 kHz PWM with dv/dt of 30 V/ns are shown in Fig. 5(a) and (b), respectively. The pulsed output of PMT aligns with the rising and falling edges of the voltage waveform indicating the presence of PD activity at the first quadrant and third quadrant of the ac wave. PD pattern in the first and third quadrant of the ac waveform is a typical characteristic in ac waveforms due to space charge accumulation. The specimen is held at a voltage marginally greater than PDIV for short duration then the PWM generator voltage is progressively decreased until no PD is detected by the PMT. The voltage at which PD extinguishes is recorded as PDEV. This implies that once PDIV is reached, PD activity will continue until the dc SST system voltage is reduced to reach PDEV. It should be noted that for each test case, fresh winding specimens are tested until three congruent results are obtained. Premature PD activity was observed in bad samples containing air pocket defects; hence, they were eliminated from the study.

The correlation of PD characteristics with switching frequency is derived by increasing the switching frequency of test waveforms. It should be noted that the tests were performed at eight different PWM frequencies and two dv/dt cases, as listed in Table I. All the tests were performed in climate controlled lab area with ambient temperature averaging to 25 °C and at normal atmospheric pressure. More than three fresh samples were identically fabricated and tested for each case. The first test case is PWM frequency of 10 Hz. The dc-link voltage of the MF generator was progressively increased in increments of 25 V and the specimen is held at each voltage for a few seconds before the progressive increase. The voltage is increased until PD is detected by the PMT and the voltage is recorded as PDIV. The red curve in Fig. 6 represents PDIV test results. The PDIV for sub kilo-hertz PWM frequencies is found higher than kilo-hertz frequencies. At 10 kHz and above frequencies, the PDIV is 25% lower than PDIV at 100 Hz. Moreover, beyond 10 kHz, PDIV

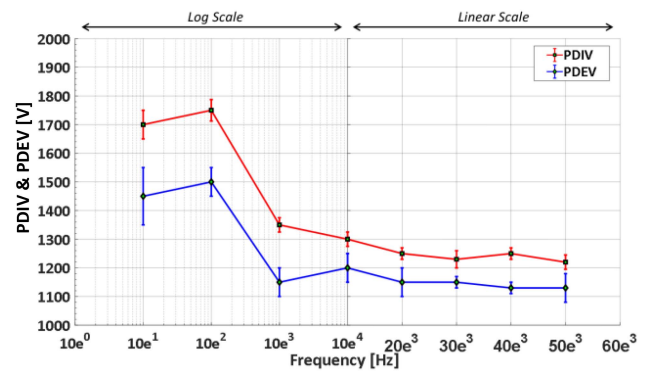


Fig. 6. PDIV and PDEV as a function of PWM frequency with $dv/dt = 30$ V/ns.

shows negligible dependence on PWM frequency. On one side, the shape of voltage waveform influences the distribution of voltage with the winding sample. On the other, the fast switching potential difference with switching transients influence the discharge physics at microscopic levels within the same conductor as well as between two adjacent conductors. Hence, marginal dependence of PDIV on switching frequency is observed when comparing the results of sub kilo-hertz low PWM frequencies with tens of kilo-hertz frequency. This can be explained by Cole-Cole model [21] that describes the inverse relationship of dielectric permittivity with frequency. However, state-of-the-art dc SST's MF transformer withstands PWM frequencies between 10 and 50 kHz, where PDIV shows no dependence on PWM frequency.

PDEV can be up to 35% below PDIV [22]; hence, the MF transformer should be designed in a such way that its absolute peak operating voltage is always below PDEV so that the discharges that are incepted during a temporary over voltage are definitely quenched at the restored operating voltage. To measure PDEV, the test sample is held at a voltage higher than PDIV, a value greater than 25% over PDEV is used in this case and then the dc-link voltage is progressively decreased

at 5–10 V intervals until the pulsed output of PMT disappears and $V_{PMT} = 0$ against V_{tr} . It should be noted that when V_{Tr} reaches close to PDEV, the strength of the discharge decreases considerably, which is exhibited by the lower amplitude and width of the PD pulses measured by the PMT. The PD activity also becomes aperiodic. PDEV is the voltage at which PD is completely extinguished. Therefore, PDEV is recorded at the dc-link voltage where no PD is detected by the PMT for more than a minute. The blue curve in Fig. 6 represents PDEV test results. Identical ratio between PDIV and PDEV values is obtained for all test cases. It is noted that the PDIV and PDEV in Fig. 6 are measured without considering the voltage ringing effect. This is due to the fact that voltage ringing can be limited by design.

Two dv/dt cases of 30 and 60 V/ns have been tested for PDIV and PDEV at PWM frequencies between 10 Hz and 50 kHz for both dv/dt . No variation in measured quantities was observed during the test that exhibits that PD characteristics are independent of tested dv/dt in PWM waveform. An explanation to this behavior is linked with the PWM waveform shape where voltage commutation is naturally fast due to steep voltage rising and falling edges. Although the change of dv/dt from 30 to 60 V/ns is significant from the semiconductor standpoint despite that, it was not enough to generate a difference in PD characteristics.

It is crucial to understand the PD characteristics of MF transformer windings because each PD event degrades the insulation material. In doing so, it considerably reduces the lifetime of the MF transformer. Since PD event is a function of switching frequency, the lifetime of the transformer is inversely proportional to the switching frequency. The following section highlights the lifetime characteristics of MF transformer.

IV. LIFETIME MODEL DEVELOPMENT

Each PD event degrades the insulation and reduces the lifetime. The winding specimen was subjected to repetitive PD, which degraded insulation material, creating an electric arc flashover through a pinhole defect on the surface of the insulation.

To study the lifetime characteristics of Kapton insulated foil winding, dielectric BD (life) tests were performed in the lab. Five switching frequencies between 10 and 50 kHz are selected with two dv/dt cases of 30 and 60 V/ns to maintain consistency with the PD characteristics measurement. This dv/dt and frequency combination is adequate for SiC enabled dc SST. Test setup shown in Fig. 4(a) has already been discussed in the previous section; hence, it will not be discussed again in this section. For each data point, more than three samples are tested to identify and avoid stochasticity in hand-made winding samples.

The winding sample is stress tested at square ac peak voltage 2 kV by maintaining the input voltage until dielectric BD occurs. The dielectric BD test is performed in the presence of PDs since the test voltage is beyond PDIV as tested in the previous section. The ac voltage is plotted on the oscilloscope by measuring V_{Tr} . When dielectric BD occurs, the voltage insulation between the primary and secondary side no longer exists, which can be observed by the sudden fall of measured voltage V_{tr} . At this instant,

a voltage difference is created at the current limiting resistance R_{ext} inserted between the half-bridge and the windings. This resistance limits the short circuit current to V_{BD}/R_{ext} to a safe value for the semiconductor device. At the same time, desat protection activates and ceases the switching action to protect the circuit from an arc fault. Activation of desat protection observed with the rise in measured current I_{BD} is an indication of a dielectric BD of winding insulation. The test is repeated for each operating point with new samples until three homogenous BD times are achieved. Broken down winding samples are tested under a microscope to assess the damage and identify the pinhole BD spot that remains unnoticeable by naked eye. The magnitude of damage remains small due to negligible current flow in the test circuit. The BD energy will increase when the transformer winding is loaded with current.

The electrical measurements obtained at the BD instant for 10 kHz PWM frequency are shown in Fig. 7(a) and for 50 kHz PWM frequency in Fig. 7(b). It should be noted that BD occurs either during the rising edge of the voltage, shown in Fig. 7(b), or in between the peak voltage level, shown in Fig. 7(a). This behavior is due to the unipolar nature of the PWM potential difference applied at the MF transformer winding sample, which enhances the electric field between the primary and secondary winding during the first and second quadrants of the ac waveform. During the third and fourth quadrants, the electric field decreases at the beginning of the third quadrant and increases only when the next ac cycle begins.

The BD times obtained for each test case are plotted in Fig. 8. From the plot, it is evident that dielectric BD is highly dependent on the ac frequency and follows an inversely proportional relationship with ac frequency. The BD time is significantly shorter for 50 kHz ac frequency as compared to 10 kHz ac. The test is repeated for two rise and fall dV/dT condition: 30 and 60 V/ns. MF transformer lifetime models are developed from the obtained test results, which will be discussed in the following sections. The lifetime test results obtained for ac PWM frequency of 10–50 kHz are utilized to derive a lifetime model for foil-type transformers that can extrapolate the lifetime of the winding specimen at a desired ac frequency by using one experimentally obtained lifetime test data as reference as shown in (2), where L_{f_n} is lifetime at PWM frequency n ; L_{ref} stands for the measured lifetime at a reference frequency; f_{ref} is the reference frequency at which L_{ref} is measured; f_n is the PWM frequency of interest to calculate lifetime; and k is the experimentally derived constant that is dependent on dv/dt of PWM waveform. Similar lifetime model has been derived in [10] for motor windings. The derived model shows good confidence extrapolating the lifetime of foil winding at any desired frequencies by using one experimentally obtained lifetime at set operating conditions as reference

$$L_{f_n} = L_{ref} * \left(\frac{f_{ref}}{f_n} \right)^k. \quad (2)$$

Insulation life heavily depends on the PWM frequency and follows an inverse relationship. The alternating electric fields impart stress on the insulation material. If the applied voltage is beyond PDIV, there will be inception and extinction of PDs in

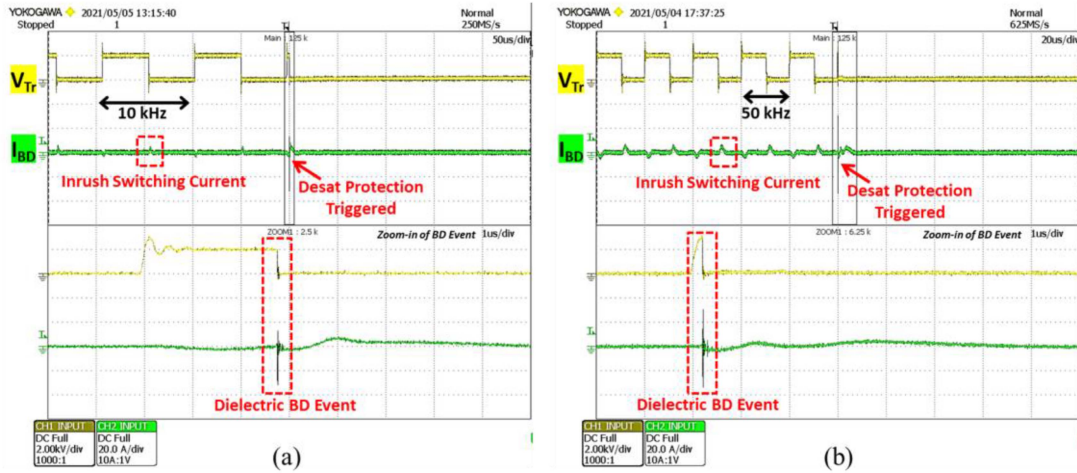


Fig. 7. Dielectric BD test waveforms with $dv/dt = 60$ V/ns. (a) 10 kHz PWM frequency. (b) 50 kHz PWM frequency.

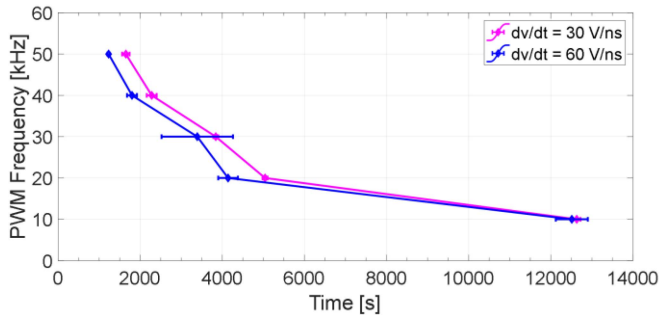


Fig. 8. BD test results for varying PWM frequency and dv/dt .

each ac cycle. Hence, the number of PD events in a unit time is proportional to the PWM frequency. This means that at higher PWM frequency, there will be more PD events in a unit time compared to a lower PWM frequency. As a consequence, at high frequency, the insulation material will suffer from higher degradation due to PD than at low PWM frequency. As a result of dielectric degradation due to PD, fastest BD is observed at 50 kHz during the test.

Additionally, the exponent of the frequency rational term k varies with dv/dt because BD is dependent on switching speed as well. The exponent of frequency rational term is obtained by curve fitting of experimentally obtained BD times. The calculated values are $k = 1.25$ for dv/dt of 30 V/ns and $k = 1.4$ for dv/dt of 60 V/ns. This establishes that the BD characteristics for the transformer winding are dependent on both switching frequency and switching speed. Faster switching speeds will negatively impact the MF transformer lifetime. Hence, an extended model is developed in the following section that considers the effect of PWM frequency and dv/dt .

Unlike PDIV, switching speed impacts the BD endurance of Kapton insulated foil winding. In Fig. 8, the magenta curve plots the results obtained at 30 V/ns switching speeds and the blue curve plots 60 V/ns switching speed. The test results for 30 V/ns show slightly better dielectric BD endurance than the faster 60 V/ns case. In the previous section, lifetime model is

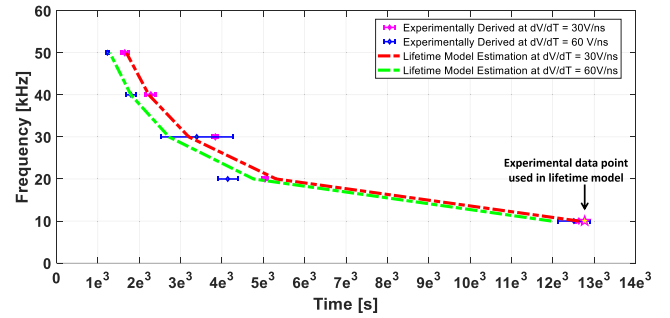


Fig. 9. Experimental lifetime test results at $dv/dt = 30$ V/ns (magenta bars); experimental lifetime test results at $dv/dt = 60$ V/ns (blue bars); extrapolated lifetime test at $dv/dt = 30$ V/ns from model (dotted red); extrapolated lifetime test at $dv/dt = 60$ V/ns from model (dotted green).

derived for varying PWM frequency at a fixed dv/dt . The experiment results conclude the dependence of insulation lifetime on switching speed, which is factored into the model with the exponential constant of the switching frequency rational. Based on the experimental data, an extended lifetime model is derived as shown in (3). This model is an extension of (2) and accounts for change in PWM frequency as well as effect of dv/dt . The extended model is obtained by curve fitting of experimental BD data and this model is used to extrapolate the lifetime in Fig. 9 using 10 kHz as f_{ref} and experimentally obtained lifetime at $dv/dt = 30$ V/ns as L_{ref}

$$L_{f_n, dv/dt T_n} = L_{ref} \left(\frac{f_{ref}}{f_n} \right)^{1.25} \left(\frac{dv/dt_{ref}}{dv/dt_n} \right)^{\frac{f_n}{128}} \quad (3)$$

The model is then used to extrapolate the lifetime at 20–50 kHz for switching speed of 30 V/ns and 10–50 kHz for 60 V/ns. The presented extrapolation boundary is between 10 and 50 kHz because that is the range of experimental test data that is used for model validation. The model tolerance is within 17% of the experimental data where the highest deviation observed from the 30 kHz test data. For the other frequencies, the model prediction lies within the experimental error boundaries, thus proving the

effectiveness of the extended lifetime model for foil-type MF transformers. The effect of peak PWM voltage is not considered because of the inability to obtain experimental results at greater than 2 kV dc-link voltages. This is because the PWM source is built using 3.3 kV device.

V. CONCLUSION

Novel findings on PD characteristics for a foil-type transformer constructed with Kapton insulation over copper foil were presented in this article. PDIV and PDEV were characterized for PWM frequencies between 10 Hz and 50 kHz. PDIV and PDEV values were about 18% higher for PWM frequencies less than 1 kHz. PD characteristics were found to have negligible dependence on dv/dt for the two dv/dt test cases.

Dielectric BD experiments were also performed in the lab with varying switching frequency and switching speed and accelerated BD tests were performed in the presence of PD. Lifetime of Kapton insulated foil winding exhibits negative exponential relationship with switching frequency and dv/dt . Transformer lifetime models were derived for varying frequency from empirically obtained test results and a unified lifetime model considering the effect of frequency and switching speed was also developed. The derived models serve as baseline for MF transformer lifetime estimation, real-time health monitoring, as well as accelerated lifetime testing for dc SSTs. The derived models provide valuable lifetime information that can support converter optimization to achieve best efficiency, power density, and reliability. Future work will continue to improve the insulation design to obtain PD free operation at high dv/dt MF PWM. The obtained lifetime model considers two electrical factors: frequency and dv/dt . Future work is also targeted to enhance the lifetime model by including the effect of voltage stress to identify the dominating factor in PD inception and winding BD. The effect of ambient conditions will also be studied along with winding to core insulation.

REFERENCES

- [1] S. Baek, Y. Du, G. Wang, and S. Bhattacharya, "Design considerations of high voltage and high frequency transformer for solid state transformer application," in *Proc. 36th Annu. Conf. IEEE Ind. Electron. Soc.*, 2010, pp. 421–426.
- [2] S. Baek and S. Bhattacharya, "Analytical modeling and implementation of a coaxially wound transformer with integrated filter inductance for isolated soft-switching DC–DC converters," *IEEE Trans. Ind. Electron.*, vol. 65, no. 3, pp. 2245–2255, Mar. 2018.
- [3] S. Zhao, Q. Li, F. C. Lee, and B. Li, "High-frequency transformer design for modular power conversion from medium-voltage AC to 400 VDC," *IEEE Trans. Power Electron.*, vol. 33, no. 9, pp. 7545–7557, Sep. 2018.
- [4] Z. Guo, R. Yu, W. Xu, X. Feng, and A. Q. Huang, "Design and optimization of a 200-kW medium-frequency transformer for medium voltage SiC PV inverters," *IEEE Trans. Power Electron.*, vol. 36, no. 9, pp. 10548–10560, Sep. 2021.
- [5] F. Guastavino and A. Dardano, "Life tests on twisted pairs in presence of partial discharges: Influence of the voltage waveform," *IEEE Trans. Dielect. Elect. Insul.*, vol. 19, no. 1, pp. 45–52, Feb. 2012.
- [6] L. Lusuardi, A. Rumi, A. Cavallini, D. Barater, and S. Nuzzo, "Partial discharge phenomena in electrical machines for the more electrical aircraft. Part II: Impact of reduced pressures and wide bandgap devices," *IEEE Access*, vol. 9, pp. 27485–27495, 2021.

- [7] B. Hu *et al.*, "A partial discharge study of medium-voltage motor winding insulation under two-level voltage pulses with high Dv/Dt ," *IEEE Open J. Power Electron.*, vol. 2, pp. 225–235, Mar. 2021, doi: [10.1109/OJPEL.2021.3069780](https://doi.org/10.1109/OJPEL.2021.3069780).
- [8] H. Xiong *et al.*, "The Ohio State University partial discharge detection platform for electric machine windings driven by PWM voltage excitation," in *Proc. IEEE Elect. Insul. Conf.*, 2019, pp. 517–520.
- [9] H. Okubo, N. Hayakawa, and G. C. Montanari, "Technical development on partial discharge measurement and electrical insulation techniques for low voltage motors driven by voltage inverters," *IEEE Trans. Dielect. Elect. Insul.*, vol. 14, no. 6, pp. 1516–1530, Dec. 2007.
- [10] D. Fabiani, G. C. Montanari, and A. Contin, "Aging acceleration of insulating materials for electrical machine windings supplied by PWM in the presence and in the absence of partial discharges," in *Proc. IEEE 7th Int. Conf. Solid Dielect.*, 2001, pp. 283–286.
- [11] B. Singh, A. J. J. Thomas, and C. Chakradharreddy, "Effect of voltage waveforms of HVDC converter transformer on lifetime characteristics," *IEEE Trans. Power Del.*, vol. 36, no. 5, pp. 3101–3108, Oct. 2021.
- [12] J. R. Laghari and P. J. Cygan, "Accelerated life studies of polyimide film under electrical and thermal multistress," in *Proc. Conf. Rec. IEEE Int. Symp. Elect. Insul.*, 1992, pp. 66–69.
- [13] R. Agarwal, S. Martin, Y. Shi, and H. Li, "High frequency transformer core loss analysis in isolated modular multilevel DC–DC converter for MVDC application," in *Proc. IEEE Energy Convers. Congr. Expo.*, 2019, pp. 6419–6423.
- [14] R. Agarwal, S. Martin, and H. Li, "Influence of phase-shifted square wave modulation on medium frequency transformer in a MMC based SST," *IEEE Access*, vol. 8, pp. 221093–221102, 2020.
- [15] R. Agarwal, S. Martin, Y. Shi, and H. Li, "High frequency transformer design for medium voltage shipboard DC–DC converter," in *Proc. IEEE Elect. Ship Technol. Symp.*, 2019, pp. 499–504.
- [16] *Amendment 1—High-Voltage Test Techniques—Partial Discharge Measurements*, IEC 60270:2000/AMD1:2015, IEC Webstore, 2015. Accessed: Jan. 11, 2022. [Online]. Available: <https://webstore.iec.ch/publication/23842>
- [17] Y. Luo *et al.*, "Partial discharge characteristics of polyimide films used in inverter-fed traction motor under different temperatures," in *Proc. Annu. Rep. Conf. Elect. Insul. Dielect. Phenom.*, 2013, pp. 809–812, doi: [10.1109/CEIDP.2013.6747072](https://doi.org/10.1109/CEIDP.2013.6747072).
- [18] P. Wang, A. Cavallini, G. C. Montanari, and G. Wu, "Effect of rise time on PD pulse features under repetitive square wave voltages," *IEEE Trans. Dielect. Elect. Insul.*, vol. 20, no. 1, pp. 245–254, Feb. 2013.
- [19] "2 Mil copper foils (.002)," Nimrod Copper. Accessed: Jan. 11, 2022. [Online]. Available: <https://www.nimrod-copper.com/product/2-mil-copper-foils-002/>
- [20] "Thorlabs - PMTSS Multialkali PMT, 185–900 nm, C-Mount threads," Accessed: Mar. 18, 2021. [Online]. Available: <https://www.thorlabs.com/thorproduct.cfm?partnumber=PMTSS>
- [21] K. S. Cole and R. H. Cole, "Dispersion and absorption in dielectrics I. Alternating current characteristics," *J. Chem. Phys.*, vol. 9, no. 4, pp. 341–351, Apr. 1941, doi: [10.1063/1.1750906](https://doi.org/10.1063/1.1750906).
- [22] A. Kuchler, *High Voltage Engineering*. New York, NY, USA: Springer Vieweg, 2018.



Rachit Agarwal (Member, IEEE) was born in Allahabad, India. He received the bachelor's degree from Uttar Pradesh Technical University, Lucknow, India, in 2014, and the M.S. and Ph.D. degrees from Florida State University, Tallahassee, FL, USA, in 2018 and 2021, respectively, all in electrical engineering.

He is currently with Aptiv, Troy, MI, USA. His research interests include WBG-based high-frequency power electronics, isolated dc–dc converters, multilevel converters, and power electronics for vehicle electrification.



Hui Li (Fellow, IEEE) received the B.S. and M.S. degrees from the Huazhong University of Science and Technology, Wuhan, China, in 1992 and 1995, respectively, and the Ph.D. degree from the University of Tennessee, Knoxville, TN, USA, in 2000, all in electrical engineering.

She is currently a Professor with the Electrical and Computer Engineering Department, Florida A&M University–Florida State University College of Engineering, Tallahassee, FL, USA. Her research interests include PV converters,

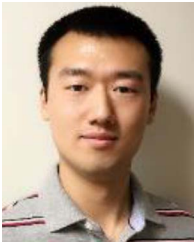
energy storage applications, and smart grid.



Peter Cheetham (Member, IEEE) received the Ph.D. degree in electrical engineering from the FAMU-FSU College of Engineering, Tallahassee, FL, USA, in 2017.

Upon graduating, he was a Postdoctoral Scholar with the Center for Advanced Power Systems, Florida State University, Tallahassee, where he is currently a Research Faculty. His research interests include high voltage engineering and high-power density superconducting devices.

Dr. Cheetham is currently a member of the IEEE's High-Voltage Testing Techniques Subcommittee and Cigre's Working Group D.1.64 on Electrical Insulation at Cryogenic Temperatures.



Zhehui Guo (Student Member, IEEE) received the B.S. and M.S. degrees in electrical engineering from the Nanjing University of Aeronautics and Astronautics, Nanjing, China, in 2015 and 2018, respectively. He is currently working toward the Ph.D. degree in electrical engineering with the Center for Advanced Power Systems, Department of Electrical and Computer Engineering, College of Engineering, Florida State University, Tallahassee, FL, USA.

His research interests include wide-bandgap device applications and high-power SiC converters.